Carbohydrate Polymers 219 (2019) 261–268

Contents lists available at ScienceDirect

Carbohydrate Polymers

journal homepage: www.elsevier.com/locate/carbpol

Chitosan-based films with incorporated supercritical CO_2 hop extract: Structural, physicochemical, and antibacterial properties

Marijan Bajić[a,*], Helena Jalšovec[b], Andrea Travan[c,d], Uroš Novak[a], Blaž Likozar[a]

[a] Department of Catalysis and Chemical Reaction Engineering, National Institute of Chemistry, Hajdrihova 19, 1000 Ljubljana, Slovenia
[b] Acies Bio d.o.o., Tehnološki park 21, 1000 Ljubljana, Slovenia
[c] Department of Life Sciences, University of Trieste, Via Licio Giorgieri 5, 34127 Trieste, Italy
[d] Biopolife s.r.l., Via Licio Giorgieri 5, 34127 Trieste, Italy

ARTICLE INFO

Keywords:
Chitosan-based films
Supercritical CO_2 hop extract
Film characterization
Antibacterial packaging

ABSTRACT

Chitosan-based films with incorporated supercritical CO_2 hop extract (HE) were developed and evaluated regarding structural, physicochemical, and antibacterial properties. The morphological and spectroscopic analyses have confirmed successful incorporation of HE into the polymer matrix, which affected films' structure and visual appearance. The presence of HE has caused a reduction in the hydrophilic character of films, but also provided a complete UV light blockage at wavelengths below 350 nm. Furthermore, a declining trend of tensile strength (from 14.4 MPa to 6.4 MPa) and Young's modulus (from 218.8 MPa to 26.9 MPa), as well as an ascending trend of elongation at break (from 10.7% to 35.1%), have been observed after the extract incorporation. The total phenolic content in the films was up to ~13 $mg_{GAE}\ g_{film}^{-1}$. Besides, the HE-loaded films exhibited antibacterial activity against foodborne pathogen *Bacillus subtilis*.

1. Introduction

Single-use plastic is broadly exploited in people's everyday life as food packaging material, especially in the form of films, wrappings, sachets, etc. Despite the fact that synthetic plastic has brought about many benefits, it became a serious environmental burden due to its unfavourable physical, chemical, and biological behaviours (Wang, Tan, Peng, Qiu, & Li, 2016). Although numerous strategies and policies have been tried out in order to facilitate the reduction of plastic pollution (Xanthos & Walker, 2017), additional efforts should be made towards the production and utilization of alternative food packaging systems (e.g. polysaccharide-based films and coatings) wherever possible (Cazón, Velazquez, Ramírez, & Vázquez, 2017).

Chitosan is a partly deacetylated derivative of naturally renewable and abundantly present chitin, mainly recovered from the exoskeleton of arthropods such as crab and shrimps (Younes & Rinaudo, 2015). It is endowed with prominent characteristics that highly depend on its average molecular weight and degree of deacetylation (Bellich, D'Agostino, Semeraro, Gamini, & Cesàro, 2016; Hosseinnejad & Jafari, 2016; Younes & Rinaudo, 2015). Thanks to its biocompatibility, biodegradability, and non-toxicity, chitosan and its derivatives are becoming notable candidates capable of producing a broad palette of materials (Muxika, Etxabide, Uranga, Guerrero, & de la Caba, 2017).

Utilization of chitosan-based materials in the food packaging industry is very promising due to chitosan's good film-forming capacity leading to a relatively simple production of films and coatings that could be incorporated by various (bio)active components (Grande-Tovar, Chaves-Lopez, Serio, Rossi, & Paparella, 2018; Wang, Qian, & Ding, 2018; Yuan, Chen, & Li, 2016). Such materials can go beyond the boundaries of traditional passive packagings by providing active antioxidant and/or antimicrobial protection and therefore shelf life extension of perishable foods (Yuan et al., 2016). So far, the incorporations of numerous (bio)active components have been attempted in order to improve antioxidant and/or antimicrobial activity of chitosan-based films, *inter alia*, essential oils (Gursoy et al., 2018; Hafsa et al., 2016; Hromiš et al., 2015; Kaya, Ravikumar et al., 2018; Priyadarshi et al., 2018; Souza et al., 2017), natural extracts (Genskowsky et al., 2015; Kalaycıoğlu, Torlak, Akın-Evingür, Özen, & Erim, 2017; Kaya, Khadem et al., 2018; Siripatrawan & Vitchayakitti, 2016; Souza et al., 2017; Sun et al., 2017), and many others (Akyuz, Kaya, Ilk et al., 2018; de Moraes Crizel et al., 2018).

Hop (*Humulus lupulus* L.) belongs to a small family of flowering plants called *Cannabaceae*, and its female inflorescences have been used through decades (Zanoli & Zavatti, 2008). The main constituents of the mature hop cones possess antioxidant and antibacterial activities that are also impersonated in the hop extracts (Kramer et al., 2015; Rój

* Corresponding author.
E-mail address: marijan.bajic@ki.si (M. Bajić).

https://doi.org/10.1016/j.carbpol.2019.05.003
Received 20 December 2018; Received in revised form 2 May 2019; Accepted 2 May 2019
Available online 07 May 2019

et al., 2015; Zanoli & Zavatti, 2008). Such findings have opened the way for the utilization of hop extracts as natural preservatives capable of extending the shelf life of perishable foods (Kramer et al., 2015; Zanoli & Zavatti, 2008). For instance, supercritical CO_2 hop extracts might be used likewise. These (usually) greenish to amber semi-fluid matter by its physical appearance under ambient conditions contain α-acids (humulone and its congeners) and β-acids (lupulone and its congeners) as the most prevalent active components, while xanthohumol and polar components are found in traces (Rój et al., 2015; Zanoli & Zavatti, 2008). Consequently, supercritical CO_2 hop extracts could be incorporated in polymer-based films as active (antioxidant/antibacterial) components, in a similar way like an ethanol-based hop extract was incorporated in the films prepared from carboxymethyl cellulose, oxidized potato starch, soy protein isolate, and gelatin in order to ameliorate their antioxidant activity (Kowalczyk & Biendl, 2016).

The aim of this study was the development and characterization of chitosan-based films with incorporated HE. In order to gain insight into the films' functionality, the prepared samples were evaluated regarding their structural (morphology, FT-IR), physicochemical (moisture content, swelling degree, total soluble matter, optical transmittance, tensile strength, elongation at break, Young's modulus, total phenolic content), and antibacterial properties.

2. Material and methods

2.1. Material

High molecular weight chitosan (310–375 kDa; ≥75% deacetylated), lactic acid (≥85%), Folin-Ciocalteu´s phenol reagent, methanol, orthophosphoric acid, and gallic acid were from Sigma-Aldrich (Steinheim, Germany), while sodium carbonate and glycerol were from Merck (Darmstadt, Germany) and Pharmachem Sušnik (Ljubljana, Slovenia), respectively. All chemicals except lactic acid were of analytical grade. Milli-Q® water was used throughout all experiments.

2.2. Chemical composition of hop extract

The chemical composition of a commercially available HE used in this study was analysed according to standard analytical methods declared by the European Brewery Convention (EBC).

2.2.1. Determination of α-acids, β-acids, and xanthohumol

The high-performance liquid chromatography (HPLC) was applied to determine the content of α-acids, β-acids, and xanthohumol in HE according to Analytica-EBC 7.7 method (European Brewery Convention, 2005). In brief, 0.5 g of HE was added to 50 mL of methanol and furthermore diluted with the same solvent 10 times. Solutions were filtered through Chromafil® Xtra PET-45/25 syringe filter (Macherey-Nagel, Düren, Germany) and injected in a 10 µL injection loop on HPLC injector. The separation was achieved using Nucleodur® 100-5 C18 ec 125 mm × 4 mm HPLC column (Macherey-Nagel, Düren, Germany). The isocratic mobile phase composed of water, methanol, and 85% aqueous solution of orthophosphoric acid in the ratio of 775/210/9 (v/v/v) was used and the detection was performed with a diode array detector (DAD) that was set at 314 nm. The quantification was carried out by the external standard ICE-4 (NATECO$_2$, Wolnzach, Germany). Xanthohumol was determined according to the same protocol, except the DAD wavelength was set at 370 nm.

2.2.2. Determination of essential oils

The essential oil content in HE was determined according to Analytica-EBC 7.10 method (European Brewery Convention, 2002). Namely, 25 ± 0.1 g of HE was mixed with 1000 mL of water in a distillation flask (V = 2000 mL), and steam distilled. The content of essential oils was measured after 3 h of distillation.

2.3. Preparation of chitosan-based films

The chitosan solution was prepared according to a slightly modified procedure outlined in Sun et al. (2017). Namely, 1.5% (w/v) of chitosan was dissolved in 1.0% (v/v) aqueous solution of lactic acid and glycerol (plasticizer) was added in the concentration of 30.0% (w/w) based on the mass of chitosan. The mixture was continuously stirred overnight on a magnetic stirrer IKA® RCT (IKA, Staufen, Germany) at 1000 rpm and room temperature (24 °C).

The raw HE was put in a glass beaker, slightly heated under the stream of warm tap water to lower its viscosity, and eventually added dropwise to chitosan solutions (100 mL) from a plastic syringe to get the initial concentrations of 0.1%, 0.5%, 1.0%, and 1.5% (w/v). The mixtures were homogenized on Ultra-Turrax® T50 (IKA, Staufen, Germany) at 6000 rpm during 2 min, vacuum-filtered through two sheets of medical gauze and left overnight to get rid of the air bubbles present in the mixtures.

Prepared film-forming solutions were cast in polyurethane Petri dishes (~0.32 mL cm^{-2}) and left in drying oven Kambič SP-55 C (Kambič, Semič, Slovenia) on a levelled surface and under continuous ventilation (at 40 °C for 48 h). The obtained films were stored under ambient conditions (relative humidity, RH 45–55%; room temperature; protected from the direct sunlight) for at least 48 h before the analysis.

The samples were labelled according to the initial extract concentrations in the film-forming solutions as follows: HE_0.0 (control sample), HE_0.1, HE_0.5, HE_1.0, and HE_1.5, i.e. the labels correspond to the films obtained from the solutions with the extract concentrations of 0.0%, 0.1%, 0.5%, 1.0%, and 1.5% (w/v), respectively.

2.4. Morphology and thickness

The morphological analysis was performed by observing the films' surfaces and cross-sections using scanning electron microscopy (SEM). The analysis was done by means of SUPRA 35 V P electron microscope (Carl Zeiss, Jena, Germany).

Thicknesses were measured from SEM images of the films' cross-sections at 10 different positions using a calibrated image analysis software ImageJ (National Institutes of Health, Bethesda, USA), and the results were averaged. This method was additionally validated by measuring the film thickness with ABS Digital Thickness Gauge (Mitutoyo, Aurora, USA).

2.5. Fourier-transform infrared spectroscopy analysis

The Fourier-transform infrared (FT-IR) spectra of HE, chitosan powder, and prepared films were recorded at room temperature at the wavenumbers ranging from 4000 cm^{-1} to 400 cm^{-1} and resolution 4 cm^{-1}, using Spectrum Two FT-IR spectrometer (PerkinElmer, Waltham, USA). The spectra were recorded in triplicates and the resulting curves were averaged.

2.6. Moisture content, swelling degree, and total soluble matter

Moisture content (*MC*), swelling degree (*SD*), and total soluble matter (*TSM*) were determined gravimetrically using a three-step method. Briefly, rectangular film samples (~1 cm^2) were weighted on the analytical balance (Kern & Sohn, Balingen, Germany) with a precision of 0.0001 g in order to get the initial mass (M_1). In the first step, the samples were dried at 105 °C for 24 h to get the initial dry mass (M_2). In the second step, the oven-dried samples with a known M_2 value were separately immersed in water (30 mL) and left at room temperature for 24 h. The water excess unabsorbed by the film specimens was superficially removed by paper wipes and the samples were weighed again to get the wet mass of the film (M_3). In the final, third step, the samples were dried once more at 105 °C for 24 h to get the final dry mass (M_4). The experiments were performed in triplicates.

MC (Eq. (1)) was defined as the percentage of mass loss due to water evaporation after drying at 105 °C for 24 h. *SD* (Eq. (2)) was defined as the percentage of mass gain due to the water absorption after dry sample immersion in water for 24 h. *TSM* (Eq. (3)) was defined as the percentage of the film dry matter that is solubilized after 24 h of immersion in water (Kowalczyk, Kordowska-Wiater, Nowak, & Baraniak, 2015).

$$MC\ (\%) = \frac{(M_1 - M_2)}{M_1} \times 100 \quad (1)$$

$$SD(\%) = \frac{(M_3 - M_2)}{M_2} \times 100 \quad (2)$$

$$TSM\ (\%) = \frac{(M_2 - M_4)}{M_2} \times 100 \quad (3)$$

2.7. Optical transmittance

The evaluation of optical transmittance was performed by inserting the film strips in a cuvette and measuring the absorbance (*A*) in the UV–vis range (250 nm–800 nm) using PerkinElmer Lambda 40 UV–vis spectrometer (PerkinElmer, Waltham, USA). The measurements were performed in triplicates at room temperature using air (i.e. an empty cuvette) as the reference, and the results were expressed as percent transmittance (%*T*) of the samples, following that $\%T = 10^{-A} \times 100$.

2.8. Mechanical properties

Mechanical characterization of chitosan-based films was performed by following the guidelines from the ASTM D 882 standard method (2002). Rectangular film samples (8 cm × 2 cm) were tested on Multitest 2.5-i universal testing machine (Mecmesin, Slinfold, UK) equipped with a 100 N load cell, at a crosshead speed of 5 mm min^{-1}. Tensile strength (*TS*) was calculated by dividing the load with the average original cross-sectional area in the gage length segment (6 cm) of the sample, elongation at break (*EB*) was calculated as the ratio between increased length after breakage and the initial gage length, whilst Young's modulus (*YM*) was calculated as the slope of the stress-strain curve linear part (considering the deformation range of 1–3%).

2.9. Total phenolic content

A crude estimation of total phenolic content (*TPC*) in chitosan-based films was determined by Folin-Ciocalteu´s (FC) phenol reagent. The pre-weighed rectangular film samples were placed in small glass vials, and the appropriate amount of water (2–3 mL) was added based on the mass of samples (10–15 mg) in order to reach the final film concentration of 5 mg mL^{-1}. FC phenol reagent and 10% (w/v) aqueous solution of Na_2CO_3 were then added successively in the amount of 10 vol% and 20 vol% based on the volume of water, respectively. The samples were incubated for 2 h under dark conditions at room temperature, and the absorbance of the solutions was measured at 765 nm using Synergy™ 2 Multi-Detection Microplate Reader (BioTek, Winooski, USA). Gallic acid was used as a standard, and the results were expressed as the mass of gallic acid equivalent (GAE) per mass of the film. The *TPC* value was followed during 51 days of film storage under ambient conditions (defined in Section 2.3). The experiment was performed in triplicates.

2.10. Antibacterial activity

The antibacterial activity of chitosan-based films was tested against the representatives of Gram-negative and Gram-positive bacterial species, namely *Escherichia coli* K12 (*E. coli*) and *Bacillus subtilis* DSM 402 (*B. subtilis*), respectively. Before the test, the film samples (~1 cm^2) were sterilised under the UV light (254 nm) on both sides for 15 min. A 100 µL of fresh bacterial culture suspension in the exponential growth phase with the OD_{600} value set to 0.5 was spread over the Luria-Bertani agar culture medium, and the samples were placed on the plate surfaces and incubated at 37 °C for 24 h. The appearance of a clear area below the films was marked as contact inhibition, while the length of clear zones around the films was measured and recorded as the inhibition zones that indicate antibacterial activity. The test was done in duplicates.

2.11. Statistical analysis

One-way analysis of variance (ANOVA) with the confidence level of 95% ($p < 0.05$) followed by Tukey's honestly significant difference post-hoc test was used to perform the statistical analysis. The results were expressed as the mean ± standard deviation.

3. Results and discussion

3.1. Chemical composition of hop extract

As already known, CO_2 is a selective solvent suited to extract non-polar hop compounds and, although the composition of resulting supercritical extracts is significantly influenced by the extraction parameters, α- and β-acids are considered to be the major constituents (Rój et al., 2015). The chemical composition of HE is presented in Table 1.

As expected, the major components were α-acids (50.20%) and β-acids (21.60%), yielding the α-acids/β-acids ratio of 2.32. The calculated α-acids/β-acids ratio was close to the value of 2.10 reported for another HE which contained 41.00% and 19.50% of α-acids and β-acids, respectively (Rój et al., 2015). The content of xanthohumol was 0.05%, while the content of essential oils was 1.38 mL per 100 g of HE (Table 1). The essential oil fraction usually contains hydrocarbons and oxygen-containing compounds (e.g. myrcene, limonene, α- and β-pinene, α-humulene, β-caryophyllene), and their ratio highly depends on the hop variety (Aberl & Coelhan, 2012).

3.2. Morphology and thickness

Predetermined amounts of HE were successfully homogenized with chitosan solutions (Fig. 1; column A). After a drying step, a set of robust, compact, transparent, and easily-peeled off chitosan-based films was obtained from the film-forming solutions (Fig. 1; column B). The films had a pale-greenish to a pale-yellowish shade that was increasing in intensity along with increasing the HE concentration (Fig. 1; column B).

As evident from Fig. 1 (column C), HE_0.0 film had a plane and compact surface without any striking cracks or pores that can indicate a discontinuity in its structure – similarly like the observations from other studies (Hafsa et al., 2016; Kaya, Khadem et al., 2018; Priyadarshi et al., 2018). A presence of unevenly distributed spots with a slightly different height level than the rest of monotonously flat surface morphology is noticeable (Fig. 1; column C). A similar situation is with the HE_0.1 film, while surface morphology became gradually rougher from HE_0.5 onwards (Fig. 1; column C). The irregularities may be attributed to a possible phase separation occurring due to the presence of essential

Table 1
Chemical composition of HE.

Component	Result
α-Acids	50.20%
β-Acids	21.60%
Xanthohumol	0.05%
Essential oils	1.38 mL/100 g

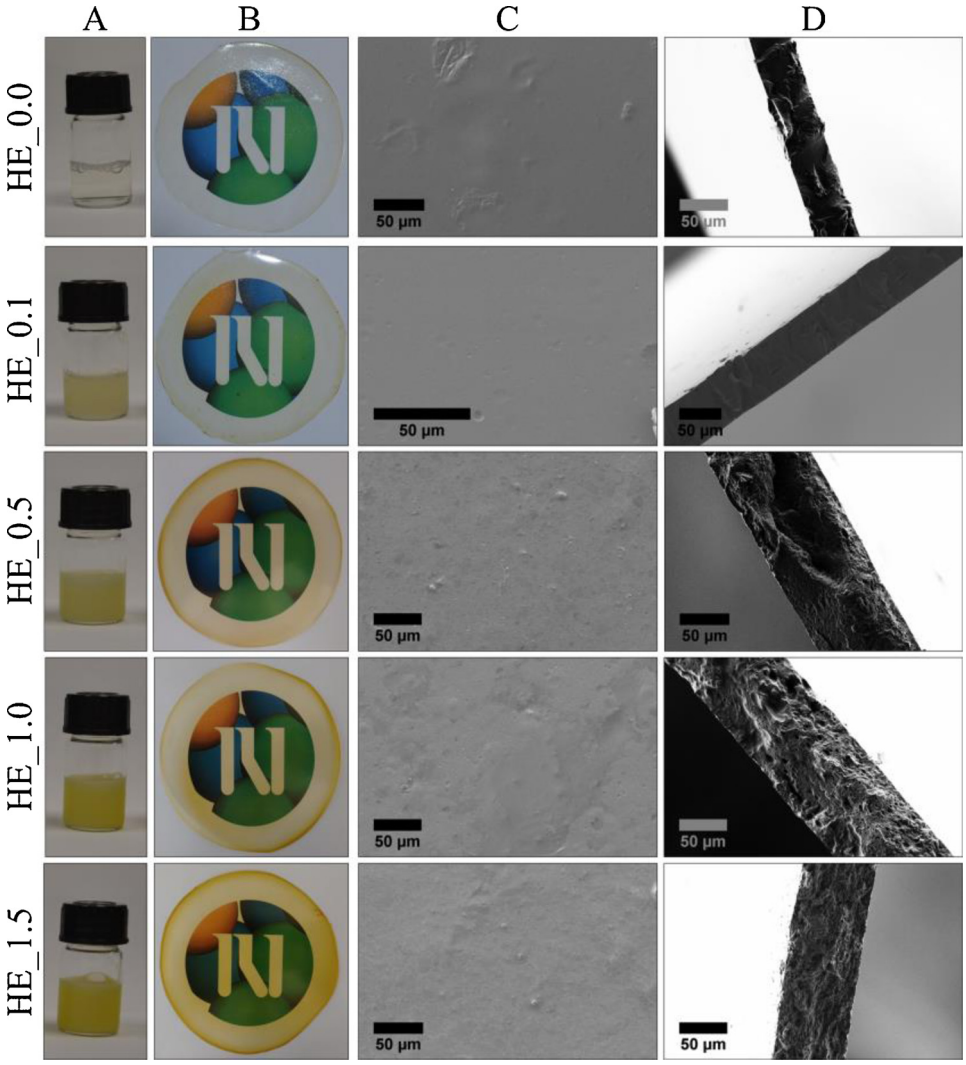

Fig. 1. Film-forming solutions and chitosan-based films: (A) physical appearance of the film-forming solutions; (B) physical appearance of the chitosan-based films; (C) SEM images of the films' surfaces, (D) SEM images of the films' cross-sections.

oils from HE that coalesced and remained embedded in the polymer matrix after the solvent evaporation. Similar conclusions have been reported for chitosan-based films containing apricot kernel essential oil (Priyadarshi et al., 2018) or eucalyptus essential oil (Hafsa et al., 2016).

In the sense of physical appearance, the cross-section morphology followed a similar pattern like the surface morphology (Fig. 1, column D). The HE_0.0 and HE_0.1 films had compact and non-porous cross-sections, whilst other samples had the cross-sections with a porous structure that was gradually increasing along with increasing the extract concentration (Fig. 1, column D). Moreover, the extract incorporation has obviously caused a significant increase in the film average thicknesses as compared to the control film since the values were 43 ± 1 μm, 59 ± 1 μm, 93 ± 2 μm, 95 ± 2 μm, and 77 ± 1 μm for HE_0.0, HE_0.1, HE_0.5, HE_1.0, and HE_1.5, respectively.

3.3. Fourier-transform infrared spectroscopy analysis

The FT-IR analysis was performed to study the possible structural interactions in chitosan-based films, and the resulting spectra are presented in Fig. 2.

The FT-IR spectrum of HE (evaluated in terms of α- and β-acids) has revealed the characteristic absorption band in the region between 3600 cm^{-1} and 3200 cm^{-1} (with a minimum at 3360 cm^{-1}) corresponding to O—H bond stretching, the adsorption peak at 2926 cm^{-1} corresponding to C—H bond stretching, and the adsorption peak at 1661 cm^{-1} corresponding to C═O bond (amide I) stretching (Fig. 2).

The FT-IR spectrum of chitosan powder has revealed the main characteristic absorptions bands and peaks which are similar to the spectra presented elsewhere (Akyuz, Kaya, Ilk et al., 2018; Kaya, Khadem et al., 2018; Leceta, Guerrero, & de la Caba, 2013): (i) a broad absorption band in the region between 3600 cm^{-1} and 3200 cm^{-1} (with a minimum at 3288 cm^{-1}) corresponding to O—H and N—H bonds stretching vibrations, (ii) a small absorption peak at 2871 cm^{-1} corresponding to C—H stretching, (iii) the absorption peak at 1651 cm^{-1} corresponding to C═O stretching (amide I), (iv) the absorption peak at 1558 cm^{-1} corresponding to N—H bending (amide II), (v) the absorption peak at 1375 cm^{-1} corresponding to C—N stretching (amide III), and the absorption peak at 1026 cm^{-1} corresponding to C—O stretching vibrations (Fig. 2). The most striking structural changes occurred after the film formation (chitosan and HE_0.0 curves in Fig. 2) could be mostly attributed to the interactions between chitosan and plasticizer (glycerol), although the protonation of the amino group in acidic condition created after the addition of lactic acid should be considered as well (Kaya, Khadem et al., 2018; Leceta et al., 2013; Matet, Heuzey, Pollet, Ajji, & Avérous, 2013).

The intermolecular interactions between chitosan and extract

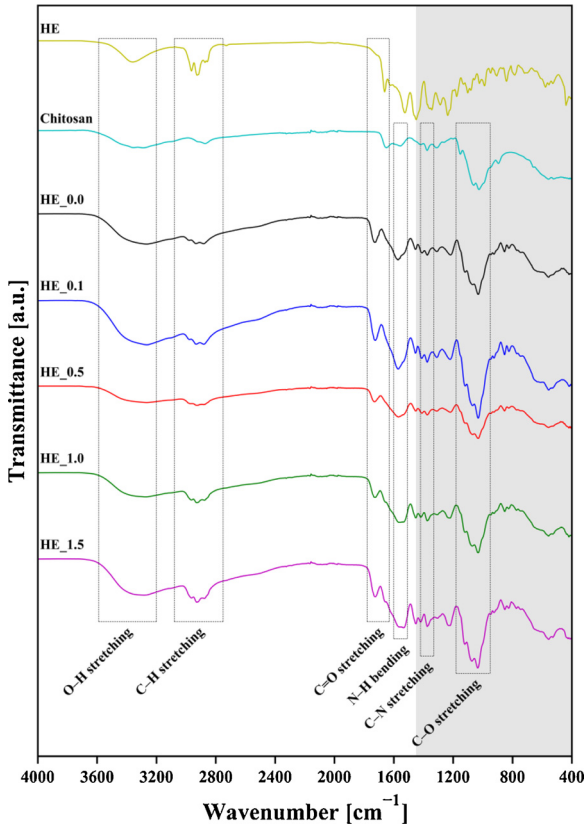

Fig. 2. FT-IR spectra of HE, chitosan powder, and chitosan-based films. The grey-shaded area represents the fingerprint region. The dashed rectangles are only for visual guidance.

components are suitable for a discussion. Namely, the major molecules present in HE have two (β-acids) or three (α-acids) proton donor atoms (in O—H groups) and proton acceptor atoms (in C=O groups), while chitosan molecule has three proton donor atoms (one in N—H and two in O—H groups) and a proton acceptor atom on acetylated monomers (in C=O groups), indicating a possible formation of hydrogen bonds between these groups (Akyuz, Kaya, Mujtaba et al., 2018). Regarding this, the most significant changes are noticeable in the spectrum of the films containing higher concentrations of the extract (HE_1.0 and HE_1.5), whereby the absorption peaks of amide I and amide II became less intense and sharp, while the intensities of broad bands corresponding to O—H and N—H bonds stretching have changed (Fig. 2). This makes us conclude that the inter- and intramolecular hydrogen bonds were probably formed between C=O groups (proton acceptors from the acids and chitosan), and N—H groups (proton donors from chitosan) or O—H groups (proton donors from the acids and chitosan). Furthermore, the peaks corresponding to C—H stretching in the HE-loaded films are getting the shape and intensity of the peak observed in the same region of HE spectrum (Fig. 2). This is especially pronounced in the spectra of HE_1.0 and HE_1.5 films and present additional proof of good incorporation of HE. Hydrogen bond-based intra- and intermolecular interactions between chitosan and incorporated active components were reported in the literature as well (Akyuz, Kaya, Ilk et al., 2018; Kaya, Khadem et al., 2018; Shen & Kamdem, 2015).

3.4. Moisture content, swelling degree, and total soluble matter

MC and *SD* imply films' capability to interact with water molecules and to keep them within the structure of the polymer matrix. Additionally, *TSM* indicates the percentage of total dry matter solubilized after the film immersion in water (Kowalczyk et al., 2015). These parameters are highly dependent on the given environmental conditions (e.g. relative humidity and temperature) as well as on the film composition and time of drying, and as such can significantly affect their functionality. Therefore, *MC*, *SD*, and *TSM* were determined and the results are summarized in Fig. 3.

As compared to the control film, all parameters have significantly decreased (with an exception for HE_0.1 in regard to *TSM*). Correspondingly, *MC* has dropped from ~30% to ~15% (Fig. 3a), *SD* from ~160% to ~74% (Fig. 3b), and *TSM* from ~24% to ~16% (Fig. 3c). The reason for a decreasing trend of these parameters in the HE-loaded films could be a double-natured one: (i) the existence of intermolecular interactions between polymer and incorporated components which are taking up chitosan's functional groups and thus preventing the establishment of chitosan-water hydrogen bonding (Section 3.3), and (ii) a hydrophobic nature of the HE components. The first reason is assumed to be more significant in terms of *MC* and *SD*, while the second one is assumed to be more significant in terms of *TSM*. However, it should be taken into account that dry films were used for the determination of *SD* and *TSM*. This may affect *SD* and *TSM* because drying process may cause a diverse alteration in regard to the film composition as well as its physicochemical and structural properties (Kowalczyk et al., 2015 and ref. therein). Therefore, if non-dried films were used in the experiments, the expected values would be probably lower in the case of *SD*, i.e. higher in the case of *TSM*.

Above all, it can be concluded that the incorporation of HE has led to increasing the hydrophobic character of films. This is in close agreement with conclusions made after the incorporation of other

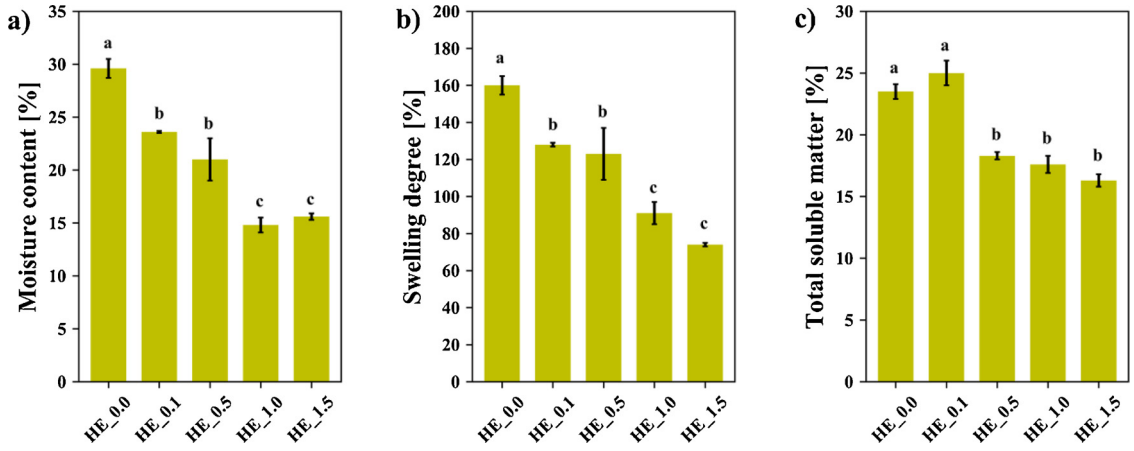

Fig. 3. Moisture content, swelling degree, and total soluble matter of chitosan-based films: a) moisture content; b) swelling degree; c) total soluble matter. The samples with different letters have significantly different mean values ($p < 0.05$).

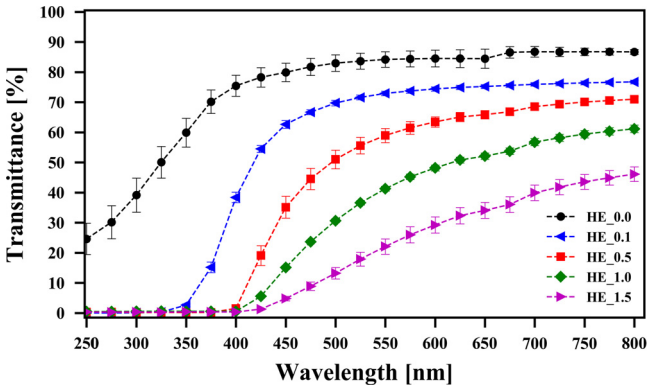

Fig. 4. Optical transmittance of chitosan-based films in the UV–vis wavelength range.

hydrophobic components such as essential oils stemming from different parts of false flax (Gursoy et al., 2018), eucalyptus (Hafsa et al., 2016), or apricot (Priyadarshi et al., 2018).

3.5. Optical transmittance

Satisfying UV and visible light barrier capabilities of chitosan-based films is a crucial property for the protection of foods containing compounds with a poor photostability (Duncan & Chang, 2012). Furthermore, the optical properties and/or physical appearance under the visible spectrum can significantly affect consumer acceptance (Akyuz, Kaya, Mujtaba et al., 2018). The light transmittance of developed chitosan-based films was measured in the UV–vis wavelength range, and the acquired results are shown in Fig. 4.

The values of light transmittance in the UV range ($\leq$400 nm) have revealed that HE_0.0 had the highest transparency – between 24.6% (at 250 nm) and 75.5% (at 400 nm). On the other side, the extract incorporation has affected optical transmittance of the films. The samples HE_0.5, HE_1.0, and HE_1.5 completely blocked the light at wavelengths between 250 nm and 400 nm, while HE_0.1 completely blocked the light at wavelengths below 350 nm and allowed transmission of 38.4% at 400 nm (Fig. 4). The observed reduction can be attributed to α-and β-acids which are capable of absorbing light in the UV range (Egts, Durben, Dixson, & Zehfus, 2012; Kowalczyk & Biendl, 2016). This trend is also in line with previously published data reporting reduction of the light transmittance in the UV range after the incorporation of ethanol-based hop extract (Kowalczyk & Biendl, 2016), turmeric extract (Kalaycıoğlu et al., 2017), or hydro-alcoholic extracts obtained from ginger, rosemary, sage, black tea, green tea, and kenaf leaves (Souza et al., 2017).

A declining trend continued in the visible region where the extract incorporation has caused a significant transmittance reduction in the wavelength range above 400 nm (Fig. 4). The maximal transmittances measured at 800 nm were 86.7%, 76.8%, 71.0%, 61.2%, and 46.1% for HE_0.0, HE_0.1, HE_0.5, HE_1.0, and HE_1.5, respectively (Fig. 4). The reduction in optical transmittance is a common case after the incorporation of active components in chitosan-based films (Akyuz, Kaya, Ilk et al., 2018; Gursoy et al., 2018; Kalaycıoğlu et al., 2017; Kaya, Khadem et al., 2018).

Due to a relatively high light adsorption capacity, the application of chitosan-based films with incorporated HE could be very effective in preventing the light-induced formation of harmful substances in food. As such, they might find the usage in packagings that are specifically designed to block the light at the most damaging wavelengths (Duncan & Chang, 2012).

3.6. Mechanical properties

Satisfying mechanical properties are crucial in providing films' integrity during the logistic processes and storage and thereby in preventing food deterioration due to packaging breakdown (Priyadarshi et al., 2018). The mechanical properties of developed chitosan-based films were evaluated regarding *TS*, *EB*, and *YM* (Fig. 5).

The evaluated samples have displayed *TS* that was spanning from 6.4 MPa to 14.4 MPa (Fig. 5a). Moreover, the HE-loaded films shown a significant downtrend in *TS* as compared to the control film (Fig. 5a). Plastic deformation was also observed for all samples since they were capable of lengthening to a considerable extent, i.e. *EB* was spanning from 10.7% to 35.1% (Fig. 5b). The evaluation of *YM* has revealed a significant decline of this parameter, namely from 218.8 MPa for the control film to 26.9 MPa for the film containing the highest concentration of HE (Fig. 5c).

The presence of HE caused a reduction in the films' resistance and stiffness (Fig. 5a and c), as well as the amelioration of their elongation capabilities (Fig. 5b). These experimental pieces of evidence suggest that the establishment of interactions between the extract components and chitosan (Section 3.3) caused a decrease of the intermolecular interactions between chitosan macromolecules, thus acting as a plasticizer by improving the chain mobility and overall film flexibility (Gursoy et al., 2018; Kaya, Ravikumar et al., 2018).

3.7. Total phenolic content

It has been proven that hop extract is able to scavenge oxidation inducers even after its incorporation in the polymeric matrix

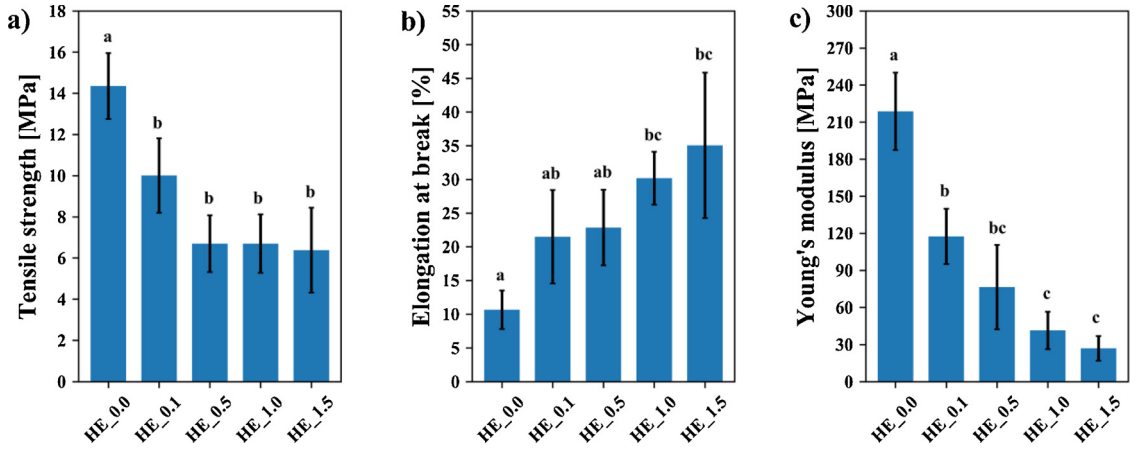

Fig. 5. Mechanical properties of chitosan-based films: a) tensile strength; b) elongation at break; c) Young's modulus. The samples with different letters have significantly different mean values ($p < 0.05$).

Table 2
Antibacterial activity of chitosan-based films against *E. coli* and *B. subtilis*.

Microorganism	Film sample	Inhibition zone [mm]	Contact inhibition
E. coli	HE_0.0	0.0 ± 0.0	+
	HE_0.1	0.0 ± 0.0	+
	HE_0.5	0.0 ± 0.0	+
	HE_1.0	0.0 ± 0.0	+
	HE_1.5	0.0 ± 0.0	+
B. subtilis	HE_0.0	0.0 ± 0.0	+
	HE_0.1	1.4 ± 0.5	+
	HE_0.5	2.5 ± 0.5	+
	HE_1.0	2.9 ± 0.9	+
	HE_1.5	3.0 ± 1.0	+

(Kowalczyk & Biendl, 2016). Keeping in mind that the antioxidant, as well as antimicrobial activities of edible films, could be in correlation with *TPC* (Hafsa et al., 2016; Kowalczyk & Biendl, 2016; Siripatrawan & Vitchayakitti, 2016), this parameter was measured and its value had been monitoring during storage of the film samples under ambient conditions (Supplementary data, Fig. S1).

A *TPC* in the control film determined at the beginning of the experiment was 0.6 $mg_{GAE}\ g_{film}^{-1}$, which is similar to the values in chitosan-based films reported in the literature (Hafsa et al., 2016; Siripatrawan & Vitchayakitti, 2016). A small overestimation of *TPC* in control film is probably due to the reaction of FC reagent with $–NH_2$ groups present in chitosan molecules (Ikawa, Schaper, Dollard, & Sasner, 2003). The *TPC* value in HE_0.1 was a little bit higher as compared to the control film (1.5 $mg_{GAE}\ g_{film}^{-1}$), while the values for other samples were significantly higher, ranging from 7.0 $mg_{GAE}\ g_{film}^{-1}$ (HE_0.5) to 12.7 $mg_{GAE}\ g_{film}^{-1}$ (HE_1.5) (Supplementary data, Fig. S1). By comparison, the chitosan-based films containing 2.5% of propolis extract (Siripatrawan & Vitchayakitti, 2016), 1.0% of maqui berry extract (Genskowsky et al., 2015), and 1.0% of eucalyptus essential oil (Hafsa et al., 2016), had *TPC* values of 4.2 $mg_{GAE}\ g_{film}^{-1}$, 8.4 $mg_{GAE}\ g_{film}^{-1}$, and 10.0 $mg_{GAE}\ g_{film}^{-1}$, respectively.

After 12 days of storage under ambient conditions, *TPC* in the HE-loaded films decreased by roughly 57 ± 3% of the initial value (Supplementary data, Fig. S1). This might be associated with the oxidative degradation of α- and β-acids to humulinones and hulupones (Taniguchi, Matsukura, Ozaki, Nishimura, & Shindo, 2013). For example, a *TPC* in the chitosan-based films with incorporated tea polyphenols decreased by ~30% after 20 days of storage (Wang, Dong, Men, Tong, & Zhou, 2013).

3.8. Antibacterial activity

Antibacterial activity of chitosan-based films is of great importance for the protection and shelf life extension of perishable foods (Priyadarshi et al., 2018). This property was evaluated against two foodborne pathogens representing Gram-negative (*E. coli*) and Gram-positive (*B. subtilis*) bacterial species, where differences in the cell membrane composition are of the key significance. The results indicating a possible presence of inhibition zones and contact inhibition are summarized in Table 2.

The growth of microorganisms was inhibited below all film samples, which indicates the existence of a contact inhibition for both bacterial species (Table 2). Apart from the contact inhibition, there were no clear growth inhibition zones of *E. coli* observed around the films (Table 2). On the contrary, even the incorporation of HE at the lowest concentration caused growth inhibition of *B. subtilis* that manifests itself as a clear zone around the film. The measured inhibition zones in the case of *B. subtilis* were increasing along with the HE concentration in chitosan-based films, whereby the values were ranging from 1.4 mm to 3.0 mm (Table 2).

These findings are generally in line with other studies reporting that Gram-negative are highly resistant, while Gram-positive bacteria are highly susceptible to the inhibition induced by hop extract active components (Kramer et al., 2015; Rój et al., 2015). The inhibition of *B. subtilis* is presumably caused by the interference of the active components with the cytoplasmic membrane, which promotes its leakage (Teuber & Schmalreck, 1973). It has been reported that this could result in the inhibition of active transport of sugars and amino acids, and consequently in the inhibition of cellular respiration and synthesis of proteins, RNA, and DNA (Teuber & Schmalreck, 1973). In the context of *B. subtilis*, it is also worth mentioning that β-acids have stronger inhibitory potential then α-acids (Kramer et al., 2015; Teuber & Schmalreck, 1973).

4. Conclusions

The hop plant is a rich source of compounds with prominent antioxidant and antibacterial activity, and hence the hop extracts have an irrefutable potential to be used as active components in the materials intended for the packaging and shelf life extension of perishable foods.

The current study has examined a possibility for the utilization of a relatively cheap, commercially available, and food-grade HE in the preparation of chitosan-based films with advanced properties. The evaluation of developed films has revealed that their properties can be tailored in terms of moisture content, swelling degree, total soluble matter, light barrier capabilities, strength, elongation, stiffness, and total phenolic content by adding a proper amount of HE. Besides, Gram-positive foodborne pathogen *B. subtilis* was susceptible to HE-loaded films, which indicates films' antibacterial activity.

However, in order to gain higher industrial relevance of developed chitosan-based films and to enable their commercial exploitation as efficient and eco-friendly packaging materials, further analyses and optimization are necessary. This primarily applies to the films' biodegradability and gas permeability as well as the release of active components and their potential side effects on the organoleptic properties of food.

Acknowledgements

This work was facilitated with the financial support provided by the BioApp project (Interreg V-A Italy-Slovenia 2014-2020). Tina Ročnik, Ana Oberlintner, and Ana Bjelić (National Institute of Chemistry, Ljubljana, Slovenia) are highly acknowledged for their help during the experimental work, whilst Francesca Scognamiglio (University of Trieste, Trieste, Italy) and Massimiliano Borgogna (Biopolife, Trieste, Italy) are acknowledged for determination of the mechanical properties.

Appendix A. Supplementary data

Supplementary material related to this article can be found, in the online version, at doi:https://doi.org/10.1016/j.carbpol.2019.05.003.

References

Aberl, A., & Coelhan, M. (2012). Determination of volatile compounds in different hop varieties by headspace-trap GC/MS – In comparison with conventional hop essential oil analysis. *Journal of Agricultural and Food Chemistry, 60*(11), 2785–2792.

Akyuz, L., Kaya, M., Ilk, S., Cakmak, Y. S., Salaberria, A. M., Labidi, J., et al. (2018). Effect of different animal fat and plant oil additives on physicochemical, mechanical, antimicrobial and antioxidant properties of chitosan films. *International Journal of Biological Macromolecules, 111*, 475–484.

Akyuz, L., Kaya, M., Mujtaba, M., Ilk, S., Sargin, I., Salaberria, A. M., et al. (2018). Supplementing capsaicin with chitosan-based films enhanced the anti-quorum sensing, antimicrobial, antioxidant, transparency, elasticity and hydrophobicity. *International Journal of Biological Macromolecules, 115*, 438–446.

ASTM International (2002). *Designation D 882: "Standard test method for tensile properties of thin plastic sheeting"*. 10.

Bellich, B., D'Agostino, I., Semeraro, S., Gamini, A., & Cesàro, A. (2016). "The good, the bad and the ugly" of chitosans. *Marine Drugs, 14*(5), 99.

Cazón, P., Velazquez, G., Ramírez, J. A., & Vázquez, M. (2017). Polysaccharide-based films and coatings for food packaging: A review. *Food Hydrocolloids, 68*, 136–148.
de Moraes Crizel, T., de Oliveira Rios, A. D., Alves, V., Bandarra, N., Moldão-Martins, M., & Hickmann Flôres, S. (2018). Active food packaging prepared with chitosan and olive pomace. *Food Hydrocolloids, 74*, 139–150.
Duncan, S. E., & Chang, H. H. (2012). Implications of light energy on food quality and packaging selection. In J. Henry (Ed.). *Advances in food and nutrition research* (pp. 25–73). Waltham: Academic Press.
Egts, H., Durben, D. J., Dixson, J. A., & Zehfus, M. H. (2012). A multicomponent UV analysis of α- and β-acids in hops. *Journal of Chemical Education, 89*(1), 117–120.
European Brewery Convention (2002). *Analytica-EBC, section 7 – hops, method 7.10, hop oil content of hops and hop products.* Nürnberg, Germany: Fachverlag Hans Carl.
European Brewery Convention (2005). *Analytica-EBC, section 7 – Hops, method 7.7, α- and β-acids in hops and hop products by HPLC.* Nürnberg, Germany: Fachverlag Hans Carl.
Genskowsky, E., Puente, L. A., Pérez-Álvarez, J. A., Fernandez-Lopez, J., Muñoz, L. A., & Viuda-Martos, M. (2015). Assessment of antibacterial and antioxidant properties of chitosan edible films incorporated with maqui berry (*Aristotelia chilensis*). *LWT – Food Science and Technology, 64*(2), 1057–1062.
Grande-Tovar, C. D., Chaves-Lopez, C., Serio, A., Rossi, C., & Paparella, A. (2018). Chitosan coatings enriched with essential oils: Effects on fungi involve in fruit decay and mechanisms of action. *Trends in Food Science and Technology, 78*, 61–71.
Gursoy, M., Sargin, I., Mujtaba, M., Akyuz, B., Ilk, S., Akyuz, L., et al. (2018). False flax (*Camelina sativa*) seed oil as suitable ingredient for the enhancement of physico-chemical and biological properties of chitosan films. *International Journal of Biological Macromolecules, 114*, 1224–1232.
Hafsa, J., Smach, M.ali, Ben Khedher, M. R., Charfeddine, B., Limem, K., Majdoub, H., et al. (2016). Physical, antioxidant and antimicrobial properties of chitosan films containing *Eucalyptus globulus* essential oil. *LWT – Food Science and Technology, 68*, 356–364.
Hosseinnejad, M., & Jafari, S. M. (2016). Evaluation of different factors affecting antimicrobial properties of chitosan. *International Journal of Biological Macromolecules, 85*, 467–475.
Hromiš, N. M., Lazić, V. L., Markov, S. L., Vaštag, Ž. G., Popović, S. Z., Šuput, D. Z., et al. (2015). Optimization of chitosan biofilm properties by addition of caraway essential oil and beeswax. *Journal of Food Engineering, 158*, 86–93.
Ikawa, M., Schaper, T. D., Dollard, C. A., & Sasner, J. J. (2003). Utilization of Folin–Ciocalteu phenol reagent for the detection of certain nitrogen compounds. *Journal of Agricultural and Food Chemistry, 51*(7), 1811–1815.
Kalaycıoğlu, Z., Torlak, E., Akın-Evingür, G., Özen, İ., & Erim, F. B. (2017). Antimicrobial and physical properties of chitosan films incorporated with turmeric extract. *International Journal of Biological Macromolecules, 101*, 882–888.
Kaya, M., Khadem, S., Cakmak, Y. S., Mujtaba, M., Ilk, S., Akyuz, L., et al. (2018). Antioxidative and antimicrobial edible chitosan films blended with stem, leaf and seed extracts of *Pistacia terebinthus* for active food packaging. *RSC Advances, 8*, 3941–3950.
Kaya, M., Ravikumar, P., Ilk, S., Mujtaba, M., Akyuz, L., Labidi, J., et al. (2018). Production and characterization of chitosan based edible films from *Berberis crataegina*'s fruit extract and seed oil. *Innovative Food Science and Emerging Technologies, 45*, 287–297.
Kowalczyk, D., & Biendl, M. (2016). Physicochemical and antioxidant properties of biopolymer/candelilla wax emulsion films containing hop extract – A comparative study. *Food Hydrocolloids, 60*, 384–392.
Kowalczyk, D., Kordowska-Wiater, M., Nowak, J., & Baraniak, B. (2015). Characterization of films based on chitosan lactate and its blends with oxidized starch and gelatin. *International Journal of Biological Macromolecules, 77*, 350–359.
Kramer, B., Thielmann, J., Hickisch, A., Muranyi, P., Wunderlich, J., & Hauser, C. (2015). Antimicrobial activity of hop extracts against foodborne pathogens for meat applications. *Journal of Applied Microbiology, 118*, 648–657.
Leceta, I., Guerrero, P., & de la Caba, K. (2013). Functional properties of chitosan-based films. *Carbohydrate Polymers, 93*(1), 339–346.
Matet, M., Heuzey, M. C., Pollet, E., Ajji, A., & Avérous, L. (2013). Innovative thermoplastic chitosan obtained by thermo-mechanical mixing with polyol plasticizers. *Carbohydrate Polymers, 95*(1), 241–251.
Muxika, A., Etxabide, A., Uranga, J., Guerrero, P., & de la Caba, K. (2017). Chitosan as a bioactive polymer: Processing, properties and applications. *International Journal of Biological Macromolecules, 105*(2), 1358–1368.
Priyadarshi, R., Sauraj Kumar, B., Deeba, F., Kulshreshtha, A., & Negi, Y. S. (2018). Chitosan films incorporated with Apricot (*Prunus armeniaca*) kernel essential oil as an active food packaging material. *Food Hydrocolloids, 85*, 158–166.
Rój, E., Tadić, V. M., Mišić, D., Žižović, I., Arsić, I., Dobrzyńska-Inger, A., et al. (2015). Supercritical carbon dioxide hops extracts with antimicrobial properties. *Open Chemistry, 13*(1), 1157–1171.
Shen, Z., & Kamdem, D. P. (2015). Development and characterization of biodegradable chitosan films containing two essential oils. *International Journal of Biological Macromolecules, 74*, 289–296.
Siripatrawan, U., & Vitchayakitti, W. (2016). Improving functional properties of chitosan films as active food packaging by incorporating with propolis. *Food Hydrocolloids, 61*, 695–702.
Souza, V. G. L., Fernando, A. L., Pires, J. R. A., Rodrigues, P. F., Lopes, A. A. S., & Fernandes, F. M. B. (2017). Physical properties of chitosan films incorporated with natural antioxidants. *Industrial Crops and Products, 107*, 565–572.
Sun, L., Sun, J., Chen, L., Niu, P., Yang, X., & Guo, Y. (2017). Preparation and characterization of chitosan film incorporated with thinned young apple polyphenols as an active packaging material. *Carbohydrate Polymers, 163*, 81–91.
Taniguchi, Y., Matsukura, Y., Ozaki, H., Nishimura, K., & Shindo, K. (2013). Identification and quantification of the oxidation products derived from α-acids and β-acids during storage of hops (*Humulus lupulus* L.). *Journal of Agricultural and Food Chemistry, 61*(12), 3121–3130.
Teuber, M., & Schmalreck, A. F. (1973). Membrane leakage in *Bacillus subtilis* 168 induced by the hop constituents lupulone, humulone, isohumulone and humulinic acid. *Archives of Microbiology, 94*(2), 159–171.
Wang, H., Qian, J., & Ding, F. (2018). Emerging chitosan-based films for food packaging applications. *Journal of Agricultural and Food Chemistry, 66*(2), 395–413.
Wang, J., Tan, Z., Peng, J., Qiu, Q., & Li, M. (2016). The behaviors of microplastics in the marine environment. *Marine Environmental Research, 113*, 7–17.
Wang, L., Dong, Y., Men, H., Tong, J., & Zhou, J. (2013). Preparation and characterization of active films based on chitosan incorporated tea polyphenols. *Food Hydrocolloids*.
Xanthos, D., & Walker, T. R. (2017). International policies to reduce plastic marine pollution from single-use plastics (plastic bags and microbeads): A review. *Marine Pollution Bulletin, 118*(1–2), 17–26.
Younes, I., & Rinaudo, M. (2015). Chitin and chitosan preparation from marine sources. Structure, properties and applications. *Marine Drugs, 13*(3), 1133–1174.
Yuan, G., Chen, X., & Li, D. (2016). Chitosan films and coatings containing essential oils: The antioxidant and antimicrobial activity, and application in food systems. *Food Research International, 89*, 117–128.
Zanoli, P., & Zavatti, M. (2008). Pharmacognostic and pharmacological profile of *Humulus lupulus* L. *Journal of Ethnopharmacology, 116*(3), 383–396.